

Article

# Optimization of Split Transmitter-Receiver Digital Nonlinearity Compensation in Bi-Directional Raman Unrepeated System

Qiang Zheng <sup>1</sup>, Zhilin Yuan <sup>1</sup>, Yuan Li <sup>2</sup> and Wei Li <sup>1,\*</sup>

<sup>1</sup> Wuhan National Laboratory for Optoelectronics, Huazhong University of Science and Technology, Wuhan 430074, China; zheng\_qiang@foxmail.com (Q.Z.); zhilin\_yuan@accelink.com (Z.Y.)

<sup>2</sup> Department of Computer Science, Central China Normal University, Wuhan 430079, China; yuanli@mail.ccnu.edu.cn

\* Correspondence: weilee@hust.edu.cn; Tel.: +86-8779225-807

Received: 7 May 2018; Accepted: 8 June 2018; Published: 13 June 2018



**Abstract:** A theoretical model of the nonlinear signal-to-noise interaction (NSNI) in a bi-directional Raman amplified system with receiver-side digital back-propagation (DBP) or split-DBP is given, which is helpful for the design of such a system. In the proposed model, the distributed Raman gain and the spontaneous Raman scattering are taken into account. The results of the theoretical calculation are compared with the results of transmission simulations, which indicates that the theoretical model matches well with the results of simulations when the pre-compensation length is less than 100 km. For the cases of pre-compensation lengths more than 100 km, the theoretical model has an error of less than 0.1 dB compared with the simulations. By using the theoretical model, the efficiency of the split-DBP is analyzed, and the results are compared with transmission simulations. Both the results of theoretical calculation and simulations show that the split-DBP can effectively mitigate the NSNI in such a system. By adopting split-DBP, with an appropriate pre-compensation length, the signal-to-noise ratio (SNR) of the signal increases by about 1 dB. In addition, the impact of the double Rayleigh scattering (DRB) is also analyzed using the proposed model, and the results show that DRB has little impact on the system.

**Keywords:** optical fiber communications; digital back-propagation; Raman amplification; nonlinear signal-to-noise interaction; nonlinearity mitigation

## 1. Introduction

In the last decade, the digital signal processing (DSP) algorithm has been developed and modern DSP-based coherent receivers can fully compensate for the linear channel impairments. Consequently, nonlinear impairments, which include mainly Kerr effects such as self-phase modulation (SPM), cross-phase modulation (XPM), and four-wave mixing (FWM), limit the transmission performance [1–3]. The digital back-propagation (DBP) algorithm is now commonly acknowledged as one of the most suitable candidates for joint linear and nonlinear impairments compensation [4–6]. In DBP, the received electric signals propagate in a simulated virtual fiber that has opposite parameters to the practical transmission fiber, and the dispersion and nonlinearity of the practical transmission fiber are eliminated. However, for the traditional DBP algorithms, noise in the system, such as Amplified Spontaneous Emission (ASE), double Rayleigh scattering (DRB), and transceiver noise, is not taken into account.

In practical optical fiber communication system, such noises in the fiber would interact with the signal through the Kerr effect, which is called nonlinear signal-to-noise interaction (NSNI). As the noises are not considered in the traditional DBP algorithm, the NSNI induced by the noises cannot be dealt with. Recently, an algorithm called stochastic DBP was proposed, in which the complex probability

method was adapted to compensate for the NSNI caused by the Erbium-doped fiber amplifiers (EDFAs) in the link [7,8]. Moreover, once the DBP algorithm was applied to the system, the noise would continue interacting with the signal during the DBP process, thus causing extra NSNI. There has been a study of the impact of the transceiver noise on the performance of DBP, which indicated that the transceiver noise would induce extra NSNI in the receiver-side DBP, thus limiting the performance of DBP [9]. To mitigate the extra NSNI, a new approach called split-DBP was proposed and studied, which involves moving a part of DBP from the receiver side to the transmitter side. By this means, part of the NSNI can be avoided and the performance is improved [10,11]. In Reference [10], D. Lavery et al. demonstrated that the split nonlinear compensation scheme is better than both post- and pre-compensation schemes in EDFA amplified systems through simulation.

Now, distributed Raman amplification is regarded as a mature and promising amplification scheme for next-generation fiber optical communication systems [12,13]. Actually, the DBP algorithm has been applied in Raman amplified unrepeated systems [14,15], but the NSNI caused by the distributed Raman gain and the spontaneous Raman scattering is in these cases ignored as well. Unlike in the EDFA amplified system, the gain in the Raman amplified systems is distributed along the fiber; consequently, the noise, which includes ASE from EDFAs, spontaneous Raman scattering, and double Rayleigh scattering, is amplified along the fiber. As a result, the NSNI in a Raman amplified system is worse than that in EDFA amplified systems.

In this paper, we theoretically deduced the NSNI in a bi-directional Raman amplified unrepeated system with receiver-side DBP and split-DBP, considering the effects of the distributed Raman gain, transceiver noise, DRB, and the spontaneous Raman scattering along the fiber. The origin of the extra NSNI in the system was studied. Theoretical analysis indicated that the extra NSNI can be effectively mitigated by adopting split-DBP. Then the performance of the split-DBP was investigated through the theoretical model and simulations, using a bi-directional Raman amplified system with 32 GBd 16QAM modulation. The impact of the DRB on the system was also studied.

## 2. Theoretical Model

Consider an unrepeated system with bi-directional Raman amplification and receiver-side DBP, as shown in Figure 1. Assuming that the nonlinear signal-to-signal (S-S) interaction is perfectly compensated by receiver-side DBP, the effective receiver signal-to-noise ratio (SNR) can be described as:

$$SNR \approx \frac{P_s}{P_{ASE} + P_{S-N}}, \tag{1}$$

where  $P_s$  is the average power of the signal;  $P_{ASE}$  is the average power of the ASE noise, including the ASE noise from EDFAs and spontaneous Raman estimation; and  $P_{S-N}$  is the power of NSNI. In the Raman amplified system, the spontaneous Raman scattering noise is generated along the fiber. Considering the spontaneous Raman scattering generated at position  $z$ , denoted by  $E_{spRs}(z)$ , it will propagate along the fiber with a length of  $L-z$  and interact with the signal, where  $L$  is the length of the whole fiber. After virtual transmission in DBP with a length of  $L-z$ , the interaction of the noise and the signal in the practical fiber is eliminated. However, the noise continues to propagate and interact with the signal in the residual virtual fiber of length  $z$ , causing the extra NSNI. The field of the extra NSNI can be described as a four-wave mixing (FWM) process [16]:

$$E_{NSNI}(z, \omega_q) = \gamma\rho(2L - z, 2L)E_s(z, \omega_i)E_s(z, \omega_j)E_{spRs}^*(z, \omega_k) + 2\gamma\rho(2L - z, 2L)E_s(z, \omega_i)E_s^*(z, \omega_k)E_{spRs}(z, \omega_j) \tag{2}$$

where the  $E_{NSNI}(z, \omega_q)$  is the field of NSNI at angular frequency  $\omega_q = \omega_i + \omega_j - \omega_k$ ,  $\gamma$  is the nonlinear coefficient,  $E_s$  is the signal field, and  $\rho(2L - z, 2L)$  is the FWM efficiency from position  $2L - z$  to  $2L$ . The latter can be written as:

$$\rho(2L - z, 2L) = \int_{2L-z}^{2L} P(\xi) e^{-i\Delta\beta} d\xi, \quad (3)$$

where  $P(\xi)$  is the normalized power profile in the fiber,  $\Delta\beta = \beta_i + \beta_j - \beta_k - \beta_g$  is the phase mismatch, and  $\beta_{i,j,k,g}$  represents the propagation constants for angular frequencies  $\omega_{i,j,k,g}$ . Note that in Equation (2) the FWM of two noise frequencies and a signal frequency is neglected because the power of the signal is much greater than the noise.

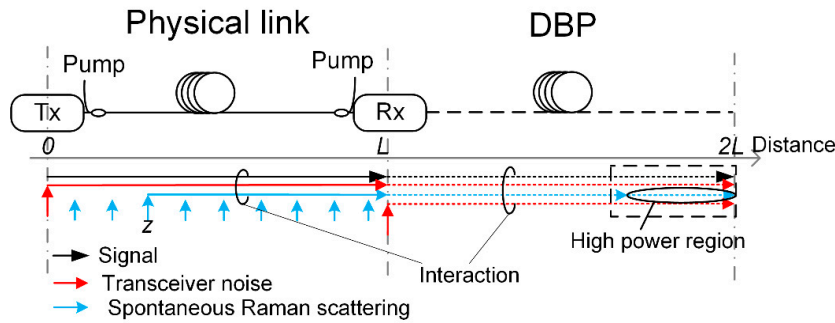


**Figure 1.** Nonlinear signal-to-noise interaction (NSNI) in a bi-directional Raman system with receiver-side digital back-propagation (DBP).

Integrating Equation (2) within the band of the signal, we can get the NSNI field at  $\omega_g$ :

$$E_{S-N}(z, \omega_g) = \iint_{\omega_{i,g} \in [-\frac{B}{2}, \frac{B}{2}]} E_{NSNI}(z, \omega_g) d\omega_i d\omega_j, \quad (4)$$

where  $B$  is the signal bandwidth. Assuming that the noise and the signal are independent random variables, the powers of the two terms in Equation (2) can be handled independently, and we can obtain the power of NSNI:

$$P_{S-N}(z) = \int \iint_{\omega_{i,g} \in [-\frac{B}{2}, \frac{B}{2}]} 3\gamma^2 |\rho(2L - z, 2L)|^2 P_s(\omega_i) P_s(\omega_j) P_{spRs}(\omega_i + \omega_j - \omega_g) d\omega_i d\omega_j d\omega_g, \quad (5)$$

$$\approx 3\gamma^2 \eta(z) P_s^2 P_{spRs}$$

where  $P_{s,spRs}(\omega)$  is the power of the signal and spontaneous Raman scattering at angular frequency  $\omega$ ,  $P_{s,spRs}$  is the average power of the signal and spontaneous Raman scattering, and  $\eta(z)$  is the nonlinear interaction coefficient, which can be written as [15]:

$$\eta(2L - z, 2L) = \iint_{\omega_{i,g} \in [-\frac{B}{2}, \frac{B}{2}]} |\rho(2L - z, 2L)|^2 d\omega_i d\omega_j, \quad (6)$$

Integrating Equation (5) along the fiber, we can obtain the total NSNI power at the end of the DBP:

$$P_{S-N} = \int_0^L 3\gamma^2 \eta(2L - z, 2L) P_s^2(z) P_{spRs}(z) dz, \quad (7)$$

Note that in Equation (7), the transceiver noise can be added into  $P_{spRs}(z)$  at positions 0 and  $L$ , for transmitter noise and receiver noise, respectively.

Because of the amplification of the forward Raman amplifier, the signal power in the front part of the fiber is very high, and in the DBP the high-power region is at the end. As in the preceding analysis, most of the overcompensation parts are in the high-power region. Thus, the overcompensation parts will produce intense extra NSNI and impair the performance of the signal. Split-DBP can effectively reduce the extra NSNI caused by DBP. When split-DBP is applied in the system, as shown in Figure 2, the NSNI includes two parts. Part one is the same as the case of the receiver-side DBP, which is caused by the overcompensation of the receiver-side DBP. Part two occurs because the NSNI in the fiber near the transmitter side is not compensated. In the same way, we can determine the total power of NSNI at the end of the receiver-side DBP by the following:

$$P_{S-N} = \int_0^l 3\gamma^2\eta(z, l)P_s^2(z)P_{spRs}(z)dz + \int_l^{2L} 3\gamma^2\eta(2L - z, 2L - l)P_s^2(z)P_{spRs}(z)dz \quad (8)$$

where  $l$  is the pre-compensation length of the transmitter-side DBP. By substituting Equations (7), (8) to (1), the final SNR of the signal can be calculated. In the practical calculations, by dividing the fiber into several blocks, the integral in Equations (7) and (8) can be simplified to the summation of the divided fiber blocks.

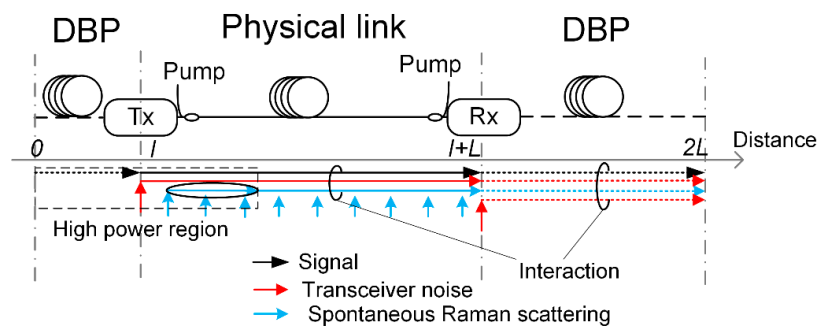


Figure 2. NSNI in a bi-directional Raman amplified system with split-DBP.

### 3. Simulation Setup

Numerical simulations were carried out with a bi-directional Raman amplified system, as shown in Figure 3. In the transmitter, a laser with a linewidth of 100 kHz and an ideal IQ modulator were assumed to generate the signal. A 32 Gbaud 16QAM signal was generated with a pseudo-random binary sequence of length  $2^{15}-1$ . The signal was sampled at eight samples/symbol and filtered by a Gaussian low-pass filter for pulse shaping. Two EDFAs, each with a noise figure of 4 dB, were deployed as the booster amplifier and pre-amplifier before the transmission link and before the coherent receiver. The transmission link was a 300-km long fiber, with attenuation coefficients of 0.2 dB/km for the signal and 0.26 dB/km for the pump, dispersion coefficient  $17 \text{ ps}\cdot\text{nm}^{-1}\cdot\text{km}^{-1}$  and nonlinear coefficient  $1.1 \text{ W}^{-1}\cdot\text{km}^{-1}$ . The signal propagation in the fiber was simulated by solving the modified nonlinear Schrödinger equation using the split-step Fourier method (SSFM) [17].

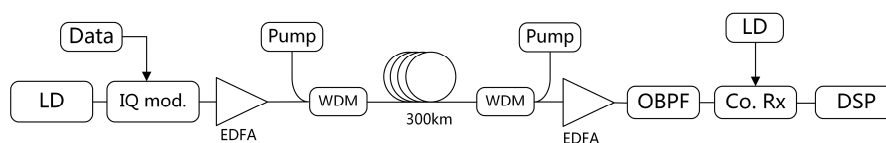


Figure 3. Simulation setup: LD: laser diode; IQ mod.: IQ modulator; OBPF: optical band-pass filter; Co. Rx: coherent receiver.

The wavelengths of the signal and pump were 1550 nm and 1455 nm, and the distributed Raman gain was calculated by solving the power coupled equations of the distributed Raman amplifier ([17], Equations (8.1.2)–(8.1.3)). In the simulation, the forward Raman pump power was set at 450 mW, and the backward Raman pump power was set at 600 mW. The relative intensity noise (RIN) transfer from the Raman pump to the signal was simulated by a time variation of the distributed Raman gain. The time variation was produced by multiplying the RIN of the pump laser and the RIN transfer function (TF) from the pump to the signal [18]. The RIN of the pump laser was set at  $-120 \text{ dBc}\cdot\text{Hz}^{-1}$ . The step size of the SSFM was 0.01 km and in each step spontaneous Raman scattering was added to the signal. After transmission, an optical band-pass filter (OBPF) was deployed with a central wavelength of 1550 nm and a bandwidth of 100 GHz. In the coherent receiver a laser with the same parameters as those in the transmitter was used as local oscillator. The photodetectors in the receiver were modeled with ideal response properties, and thermal noise and shot noise were considered. The thermal noise was modeled as white noise in the spectrum with  $10^{-12} \text{ A}\cdot\text{Hz}^{-1/2}$ . Then the received signal was down-sampled to two samples/symbol for subsequent DSP.

In the receiver, DSP carrier recovery was applied to compensate for the phase shift of the laser. Two nonlinear compensation methods were applied in the simulation: receiver-side DBP and split-DBP. To fairly compare the performance of the transmitter-side DBP and split-DBP, in the split-DBP scheme, the signal was processed by the transmitter-side DBP at two samples/symbol, and then the processed signal was up-sampled to eight samples/symbol for fiber transmission. The electrical SNR of the signal was calculated after the DSP.

## 4. Results and Discussion

### 4.1. Accuracy of the Theoretical Model

In Section 2 we gave the expression of the final SNR of the signal in a bi-directional Raman amplified system with receiver-side DBP or split-DBP. In this section, we will verify the accuracy of the model through simulation and demonstrate the efficiency of split-DBP.

First, to find the optimal pre-compensation length, different pre-compensation lengths were applied, and the SNRs of the signals were calculated using Equations (7) and (8) with different incident powers. Correspondingly, the transmission simulations were carried out with the same parameters. The SNRs of the signals in the transmission simulations were calculated using the error vector magnitude (EVM). As shown in Figure 4a, after calculating the average amplitude of each point of the signal constellation and the standard deviation of the noise, the EVM of the signal can be calculated, then the SNR of the signal can be calculated by  $\text{SNR} = 1/\text{EVM}^2$ . The simulation results were compared with the theoretical results, and both are shown in Figure 4b.

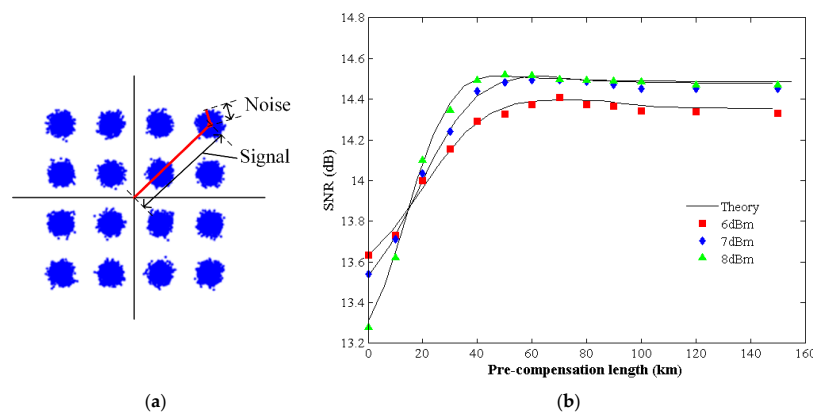


**Figure 4.** (a) The calculation method of the error vector magnitude (EVM) of the signal, (b) signal-to-noise ratio (SNR) vs. The pre-compensation length.

In Figure 4b, the black lines are the theoretical calculation results, the colorful marks are the results of simulations, and the different curves denote different incident powers. Comparing the results of theory and simulations, it can be found that the results of the theoretical calculation fit well with the simulations when the pre-compensation length was less than 100 km. When the pre-compensation length was more than 100 km, the SNR of the theoretical calculation was larger than the simulation, which we attributed to the influence of the up-sampling and the low-pass filter, which brings error to the transmitter-side DBP.

As we can see, when the pre-compensation was 0, representing the receiver-side DBP, with the incident power increasing from 6 dBm to 8 dBm, the SNR of the signal decreased. This indicates that the NSNI caused by the DBP affects the performance of the signal. When split-DBP was applied, the SNR of the signal increased first and then remained at a high level, with the pre-compensation length increasing. For different incident powers, the optimal pre-compensation lengths were all round 50 km, but had small differences, and the trend was that the optimal pre-compensation length decreased with an increase in incident power.

Then, to determine the efficiency of the split-DBP, the pre-compensation length was set to 0 and 50 km, and the SNRs of the signals were calculated with different incident powers, as well as simulations. The results are shown in Figure 5. Similarly, in this figure the black lines denote the results of the theoretical calculation and the colorful marks denote the results of the simulations. Because the pre-compensation length was less than 100 km, the results of the theoretical calculation matched well with the simulations. And we can see, by adopting split-DBP, the optimal incident power increased from 6 dBm to 8 dBm, and the maximum SNR increased by about 1 dB. This demonstrates the efficiency of NSNI mitigation of the split-DBP in the bi-directional Raman amplified system. However, we can see that when the incident power was over 8 dBm, the SNR of the signal still decreased quickly, which indicates there are other complicated nonlinear effects that impact the signal.

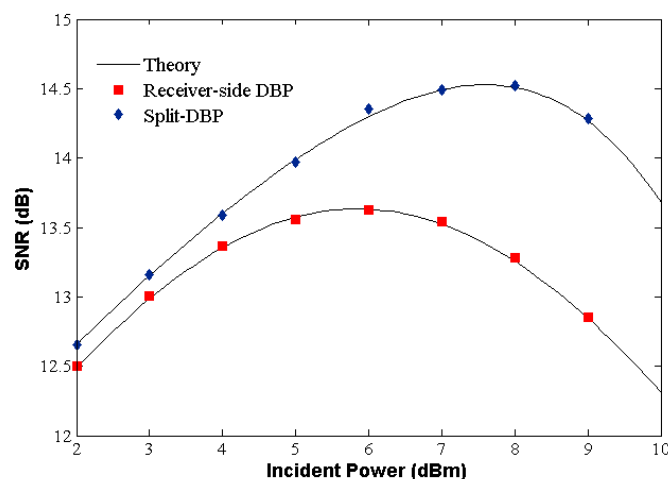


Figure 5. SNR vs. incident power.

#### 4.2. Impact of Double Rayleigh Backscattering

In the theoretical analysis and the simulation above, the DRB in the system was neglected. In this section we take the DRB into consideration, and analyze the impact of the DRB on the system. In the proposed theoretical model, we calculate the NSNI caused by the transceiver noise and spontaneous Raman scattering. These two kinds of noise can be treated as “dot” noise, which means that the noise is generated within a very small distance. However, the DRB in the system cannot be treated as the same way. It is obvious that the DRB at a point is relevant to the Raman gain and the signal power in the whole following fiber. To include the DRB to the proposed model, the DRB noise should be

converted into “dot” noise. For simplicity, we firstly calculate the average power distribution of the DRB along the fiber [19]:

$$P_{DRB}(z) = \int_z^L P_s(z') \zeta^2 \exp\left(\int_{z'}^z [-\alpha_s + g_R P_p(z'')] dz''\right) dz' \tag{9}$$

where  $P_{DRB}$  is the power of the DRB,  $\zeta$  is the Rayleigh backscattering coefficient,  $\alpha_s$  is the fiber attenuation at the wavelength of the signal,  $g_R$  is the Raman gain coefficient, and  $P_p$  is the Raman pump power. Note that in Equation (9) the consumption of the pump due to the DRB is ignored. Then the DRB noise can be generated at each point in the fiber according to its statistical distribution. In the theoretical model and simulation the DRB is treated as Gaussian additive noise. Although the exact statistical characteristic of the DRB is not very clear yet, according to the central limit theorem, the Gaussian approximation of the DRB in a small section of the fiber is acceptable.

After obtaining the power profiles of the signal and the pumps, the power profile of the DRB can be calculated using Equation (9). With the same parameters as the simulation above, we calculated the power profile of the DRB, which is shown in Figure 6. For comparison, the power profiles of the signal and the spontaneous Raman scattering are plotted in Figure 6 as well. As we can see from the figure, compared to the spontaneous Raman scattering, the DRB has higher power in the near-transmitter section, but lower power in the near-receiver section of the fiber. Because the signal power in the near-transmitter section of the fiber is much higher than that in the near-receiver section, the noise in the near-receiver side section has more severe impact on the optical signal-to-noise ratio (OSNR) of the signal. That means that the spontaneous Raman scattering is a more important noise source than the DRB. Figure 7 plots the OSNR degradation of the signal along the fiber. When only the spontaneous Raman was considered, in the near-transmitter section the OSNR of the signal decreased slowly, but in the near-receiver section of the fiber the OSNR of the signal exhibited a sharp decrease. On the other hand, in the case with only DRB, the OSNR of the signal exhibited a small drop in the near-transmitter section and decreased slowly in the rest section of the fiber. And at the end of the fiber, the OSNR of the case in which only spontaneous Raman scattering was considered is lower than the OSNR of the case with only DRB. This indicates that spontaneous Raman scattering has higher impact on the system than the DRB.

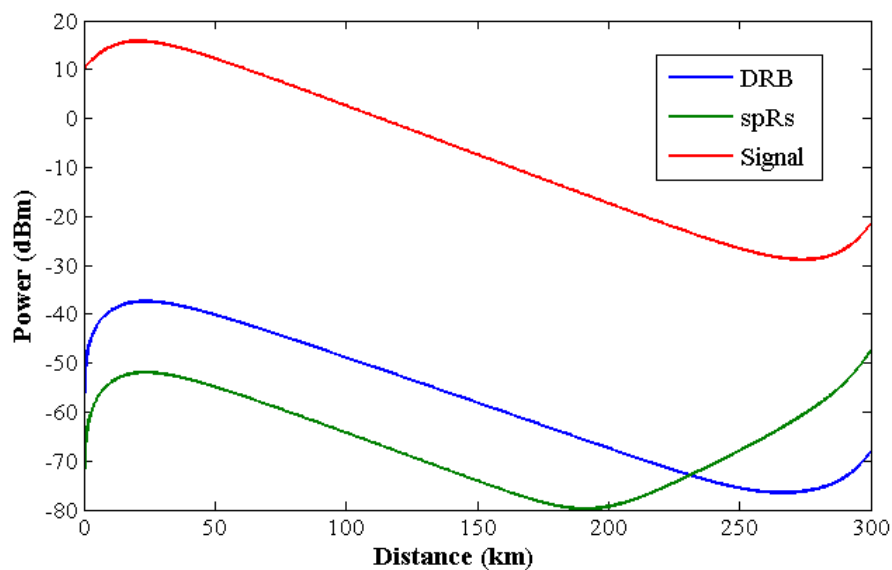
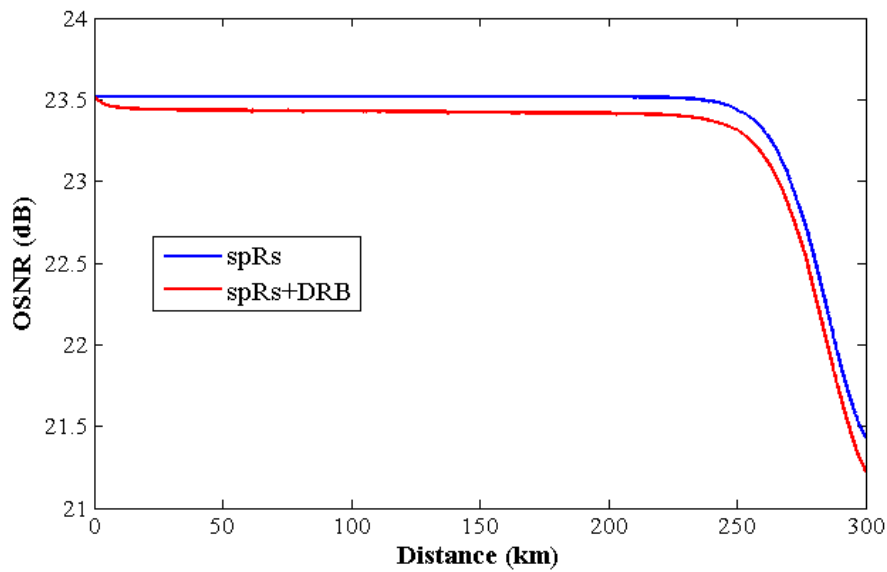
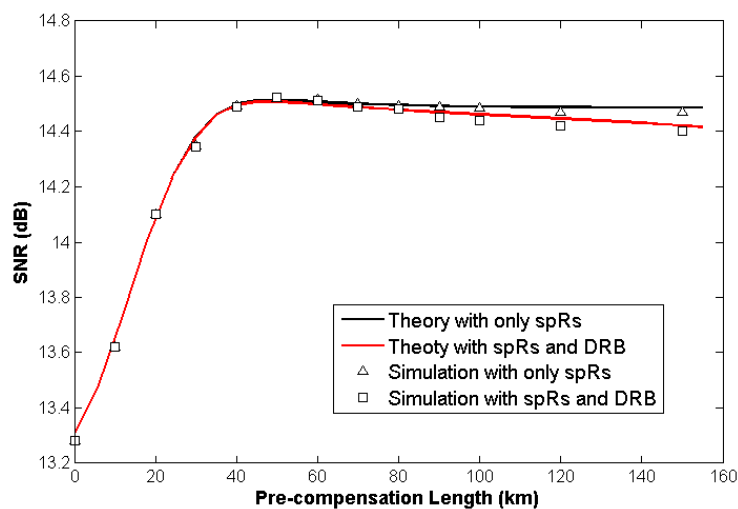


Figure 6. Power profiles of the signal, spontaneous Raman scattering (spRs), and DRB.



**Figure 7.** OSNR vs. distance, with only spontaneous Raman scattering (spRs) and with both spRs and DRB.

Next, we take the NSNI into consideration. According the analysis above, when the receiver-side DBP is applied, the noise in the near-receiver section causes more severe NSNI, because the noise in the near-receiver section is amplified in the DBP process. Thus, the NSNI caused by spontaneous Raman scattering is also higher than the NSNI caused by the DRB. To demonstrate this point, the SNRs of the signals were calculated using the proposed theoretical model with the DRB included, and the results were compared with the case in which only spontaneous Raman scattering was considered, as shown in Figure 8. From Figure 8, we can see that when the DRB was considered, the proposed model had good accuracy. When the pre-compensation length was less than 60 km, the two curves were almost coincident. With the pre-compensation length increasing over 60 km, a difference appeared and the SNR of the signal including DRB was lower than the SNR of the signal without DRB. This is because the NSNI caused by the DRB in the near-transmitter section increased. Still, the difference is small, which illustrates that the DRB has a much smaller influence on the performance of the system than spontaneous Raman scattering.



**Figure 8.** SNR vs. The pre-compensation length, with and without DRB.

## 5. Conclusions

In this paper, we theoretically deduced the NSNI in a bi-directional Raman amplified unrepeated system with receiver-side DBP and split-DBP, considering the effects of the distributed Raman gain, the spontaneous Raman scattering, and DRB. The results of the theoretical calculation were compared with the results of transmission simulations, which indicated that the theoretical model has good accuracy when the pre-compensation length is less than 100 km. Both the results of the theoretical calculation and simulations showed that the split-DBP can effectively mitigate the NSNI in such a system. By adopting split-DBP, with an appropriate pre-compensation length, the SNR of the signal increased by about 1 dB. According to the theoretical analysis, the DRB has much a smaller influence on the system than spontaneous Raman scattering. The theoretical model given in this paper is helpful in the design of a bi-directional Raman amplified system.

**Author Contributions:** Q.Z. finished writing the whole manuscript and conducted the simulations. Z.Y., Y.L., and W.L. presented the idea. Q.Z. and Z.Y. are the co-first authors.

**Funding:** This research received no external funding.

**Acknowledgments:** This work is supported by Open Foundation of China Southern Power Grid and State Key Laboratory of Optical Communication Technologies and Networks (W.R.I.) and the Accelink Technologies Company Ltd. The help of Shaohua Yu and Zhixue He from Wuhan Research Institute of Posts and Telecommunications is also acknowledged.

**Conflicts of Interest:** The authors declare no conflict of interest.

## References

1. Mohamed, A.; AliKarar, M.; Landolosi, T. DSP-based dispersion compensation: Survey and simulation. In Proceedings of the 2017 International Conference on Communication, Control, Computing and Electronics Engineering (ICCCCEE), Khartoum, Sudan, 16–18 January 2017.
2. Erdogan, A.T.; Demir, A.; Oktem, T.M. Automatic PMD compensation by unsupervised polarization diversity combining coherent receivers. *J. Light. Technol.* **2008**, *26*, 1823–1834. [[CrossRef](#)]
3. Essiambre, R.J.; Kramer, G.; Winzer, P.J.; Foschini, G.J.; Goebel, B. Capacity limits of optical fiber networks. *J. Light. Technol.* **2010**, *28*, 662–701. [[CrossRef](#)]
4. Ip, E.; Kahn, J.M. Compensation of dispersion and nonlinear impairments using digital backpropagation. *J. Light. Technol.* **2008**, *26*, 3416–3425. [[CrossRef](#)]
5. Ip, E. Nonlinear compensation using backpropagation for polarization-multiplexed transmission. *J. Light. Technol.* **2010**, *28*, 939–951. [[CrossRef](#)]
6. Maher, R.; Xu, T.; Galdino, L.; Sato, M.; Alvarado, A.; Shi, K.; Savory, S.J.; Thomsen, B.C.; Killey, R.I.; Bayvel, P. Spectrally shaped DP-16QAM super-channel transmission with multi-channel digital back-propagation. *Sci. Rep.* **2015**, *5*, 8214. [[CrossRef](#)] [[PubMed](#)]
7. Irukulapati, N.V.; Wymeersch, H.; Johannisson, P.; Agrell, E. Stochastic digital backpropagation. *IEEE Trans. Commun.* **2014**, *62*, 3956–3968. [[CrossRef](#)]
8. Irukulapati, N.V.; Marsella, D.; Johannisson, P.; Agrell, E. Stochastic digital backpropagation with residual memory compensation. *J. Light. Technol.* **2016**, *34*, 566–572. [[CrossRef](#)]
9. Galdino, L.; Semrau, D.; Lavery, D.; Saavedra, G.; Czegledi, C.B.; Agrell, E.; Killey, R.I.; Bayvel, P. On the limits of digital back-propagation in the presence of transceiver noise. *Opt. Express* **2017**, *25*, 4564–4578. [[CrossRef](#)] [[PubMed](#)]
10. Lavery, D.; Ives, D.; Liga, G.; Alvarado, A.; Savory, S.J.; Bayvel, P. The benefit of split nonlinearity compensation for single channel optical fiber communications. *IEEE Photon. Technol. Lett.* **2016**, *28*, 1803–1806. [[CrossRef](#)]
11. Lavery, D.; Maher, R.; Liga, G.; Semrau, D.; Galdino, L.; Bayvel, P. On the bandwidth dependent performance of split transmitter-receiver optical fiber nonlinearity compensation. *Opt. Express* **2017**, *25*, 4554–4563. [[CrossRef](#)] [[PubMed](#)]
12. Bromage, J. Raman amplification for fiber communications systems. *J. Light. Technol.* **2004**, *22*, 79. [[CrossRef](#)]

13. Pelouch, W.S. Raman amplification: An enabling technology for long-haul coherent transmission systems. *J. Light. Technol.* **2016**, *34*, 6–19. [[CrossRef](#)]
14. Galdino, L.; Tan, M.; Alvarado, A.; Lavery, D.; Rosa, P.; Maher, R.; Ania-Castanón, J.D.; Harper, P.; Makovejs, S.; Thomsen, B.C.; Bayvel, P. Amplification schemes and multi-channel DBP for unrepeated transmission. *J. Light. Technol.* **2016**, *34*, 2221–2227. [[CrossRef](#)]
15. Saavedra, G.; Semrau, D.; Galdino, L.; Killey, R.I.; Bayvel, P. Digital back-propagation for nonlinearity mitigation in distributed Raman amplified links. *Opt. Express* **2017**, *25*, 5431–5439. [[CrossRef](#)] [[PubMed](#)]
16. Inoue, K.; Toba, H. Fiber four-wave mixing in multi-amplifier systems with nonuniform chromatic dispersion. *J. Light. Technol.* **1995**, *13*, 88–93. [[CrossRef](#)]
17. Agrawal, G.P. *Nonlinear Fiber Optics*, 3rd ed.; Academic Press: New York, NY, USA, 2007.
18. Kalavally, V.; Rukhlenko, I.D.; Premaratne, M.; Win, T. Analytical Study of RIN Transfer in Pulse-Pumped Raman Amplifiers. *J. Light. Technol.* **2009**, *27*, 4536–4543. [[CrossRef](#)]
19. Cheng, J.; Tang, M.; Fu, S.; Shum, P.P.; Liu, D. Characterization and Optimization of Unrepeated Coherent Transmission Systems Using DRA and ROPA. *J. Light. Technol.* **2017**, *35*, 1830–1836. [[CrossRef](#)]



© 2018 by the authors. Licensee MDPI, Basel, Switzerland. This article is an open access article distributed under the terms and conditions of the Creative Commons Attribution (CC BY) license (<http://creativecommons.org/licenses/by/4.0/>).